**Jurnal Elektronika dan Telekomunikasi (JET)**, Vol. 24, No. 1, August 2024, pp. 72-79
Accredited by KEMDIKBUDRISTEK, Decree No: **158/E/KPT/2021**
doi: 10.55981/jet.596

# Performance Comparison of PID, FOPID, and NN-PID Controller for AUV Steering Problem

**Osen Fili Nami [a, *], Afif Widaryanto [a], Muhammad Putra Rasuanta [a], Tinova Pramudya [a], Muhammad Yusha Firdaus [a], Peni Laksmita Widati [a], Sakinah Puspa Anggraeni [b], Hanifah Dwiyanti [a], Maristya Rahmadiansyah [a], Michael Andreas Purwoadi [a], Sasono Rahardjo [a], Teddy Alhady Lubis [c]**

[a]*Research Center for Electronics*
*National Research and Innovation Agency of Indonesia*
*Komplek BRIN, Jl. Sangkuriang No 21, 40135*
*Bandung, Indonesia*
[b]*Research Center for Telecommunication*
*National Research and Innovation Agency of Indonesia*
*Komplek BRIN, Jl. Sangkuriang No 21, 40135*
*Bandung, Indonesia*
[c]*Research Center for Smart Mechatronics*
*National Research and Innovation Agency of Indonesia*
*Komplek BRIN, Jl. Sangkuriang No 21, 40135*
*Bandung, Indonesia*

**Abstract**

This study examines and compares three autonomous underwater vehicles (AUV) steering control techniques using the following three control algorithms: proportional-integral-derivative (PID), fractional order PID (FOPID), and neural network PID (NN-PID). This investigation aims to comprehensively understand each controller's response regarding step input scenarios, trajectory changes, and when encountering disturbances. The response analysis will evaluate the strengths and weaknesses of the controller by examining parameters such as rise time, settling time, settling min, settling max, overshoot, peak, and peak time for each controller response. The root mean square error (RMSE) technique will be applied to determine the accuracy performance of each controller strategy, allowing users to select the most suitable controller option confidently. FOPID displays the best settling time of 3.2218 seconds, while PID stands out in rise time, achieving 0.4725 seconds. The results indicate that NN-PID is the top performer as it reduces overshoot to 0.3022%. Among the three controllers tested, FOPID had the smallest RMSE value, while the NN-PID control's slower response and larger error resulted in a smaller overshoot than PID and FOPID. This factor is due to the online learning process on NN-PID, which requires time. Based on the simulation results, FOPID outperforms PID in settling time and produces the smallest error due to the inclusion of parameters λ and μ, leading to improved control performance.

**Keywords:** Autonomous Underwater Vehicles (AUV), steering, PID, FOPID, NN-PID.

## I. Introduction

Autonomous underwater vehicles (AUVs) are widely recognized for their ability to operate underwater without human intervention, making them increasingly important in various applications. AUVs are commonly used for offshore surveys, marine research, fisheries management, oceanography, and exploration of underground flooded mines [1]–[5]. However, their deployment has several challenges, such as communication, localization, and navigation in underwater environments [2]. AUVs were developed to meet the requirements of multipoint short-term synchronous offshore surveys [1]. The critical issues in underwater imaging with AUVs include the characteristics of the underwater environment, camera optics, preprocessing, image mosaicking techniques, and algorithmic processing [4]. This investigation is of great importance for marine science as it will significantly impact the exploration of natural resources [6].

AUVs are of growing importance in marine exploration, research, and industry due to their ability to operate independently and collect data in various marine environments. AUVs offer several advantages, such as their capacity to obtain high-resolution maps of the deep seafloor, a feature useful for studying seafloor morphology, geology, and ecology [7]. Moreover, it can collect various data types, including water column properties, seafloor imagery, and acoustic data [8]. Objectively, this craft can be more cost-effective than traditional research vessels due to their extended operational capabilities and greater ocean coverage [8]. Additionally, they increase safety when exploring hazardous environments, including deep-sea hydrothermal vents, by eliminating the risk to human life [7]. According to an article published in Marine Geology,

* Corresponding Author.
Email: osen001@brin.go.id
Received: October 31, 2023 ; Revised: December 30, 2023
Accepted: May 06, 2024 ; Published: August 31, 2024

forthcoming advances in AUV technology embrace novel vehicles with upgraded hovering, elongated endurance, and improved sampling capabilities [8]. Steering control systems are essential for the navigation and successful completion of missions for every autonomous vehicle. AUVs are incredibly maneuverable and can be programmed to follow precise routes or perform particular tasks. However, because of environmental disturbances, underactuated issues, system constraints, and coupling, controlling the trajectory of AUVs is challenging [9]. Therefore, a successful mission necessitates the development of navigation and motion control systems. An academic article [10] discussed the progress in developing such systems and provided initial insights into the development of navigation and motion control systems for AUVs with both automatic and manual control. Manual control is carried out in real-time by an operator via a fiber-optic cable using a joystick. Automatic control enables the AUV to move independently along a specified trajectory at a given depth and speed. The AUV also features a collision avoidance system that uses readings from a forward-facing acoustic rangefinder to estimate the time before impact based on the AUV's analytical model. Computer simulation using the analytical model was employed to assess the performance features of the devised control and navigation algorithms. Following verification of operability, preliminary tests were conducted on the AUV. During the tests, the AUV's onboard equipment and navigation system readings were recorded and compared with those of the reference system. The reference system was also employed to evaluate the developed control and navigation algorithms. Another academic study [9] offered a comprehensive examination of the complexities involved in controlling craft trajectory tracking. It assesses several models and control strategies proposed in academic literature, articulating the pros and cons of each approach and offering examples of successful AUV missions that have implemented these strategies. It assesses several models and control strategies proposed in academic literature, articulating the pros and cons of each approach and offering examples of successful AUV missions that have implemented these strategies.

The efficacy of diverse steering control approaches in AUVs is a critical research issue explored in numerous scholarly works. AUVs exhibit exceptional maneuverability and can be programmed to trace predefined courses or execute specific tasks. However, due to glitches associated with environmental factors, actuation, and system coupling, tracking the trajectory of an AUV can be quite arduous [9]. Therefore, developing efficient steering control methods is imperative for the productive operation of AUVs [11]. Other previous studies also examined various steering control methods for AUVs [9], [11]. This study presents an overview of the key aspects of control-oriented models and methodologies of control strategies employed for trajectory tracking of AUVs. The article explores different mathematical models and control strategies for underwater marine craft, including optimal, nonlinear time-invariant, adaptive, robust, and intelligent control. Successful AUV missions that have utilized these strategies are provided as examples. Another academic article cited as [12] discussed steering control methods for AUVs and proposed an improved artificial potential field algorithm aided by multisource data for AUV path planning. The study explored the utilization of a gyroscope to gauge the dimensions of the steering angle and attack angle in real time and applied Kalman filtering to the AUV's steering angle.

Additionally, [10] outlined the initial outcomes of developing AUV navigation and motion control systems. The article delved into the AUV's control system, which enables manual and automatic control. Real-time manual control is executed by the operator through a joystick via fiber-optic cable. Automatic control allows the AUV to move independently along a predefined trajectory at a specified depth and speed. Furthermore, the article examines employing computer simulation to validate the performance characteristics of the constructed control and navigation algorithms, utilizing the analytical AUV model.

Addressing the research problem of precise and efficient steering control in AUVs is crucial. Moreover, the steering system is a vital constituent of AUVs, and its nonlinear inputs, like dead zone and saturation, can drastically influence the actuator for heading control of underactuated AUVs [13]. Therefore, developing optimal control systems for AUVs' steering and depth subsystems is crucial to improving their maneuvering precision, stability, and battery life [9]. Additionally, establishing trajectory-tracking models is necessary to enhance the decision-making and intervention ability of the system [14]. Implementing decoupling algorithms and PSO-ADRC controllers can aid stable attitude stabilization control of AUVs [10]. It is crucial to address the research problem of precise and efficient steering control systems in AUVs to guarantee the necessary accuracy, reliability, and stability for accomplishing various tasks. By doing so, it is possible to enhance their overall performance and safety while reducing human intervention requirements. Improved control systems can significantly enhance AUVs' performance and safety significantly. By developing new control-oriented models, undertaking research into the estimation of unknown inputs, and exploring more innovative control strategies, the trajectory tracking of AUVs can be improved [9]. These technologies are gradually advancing, and attention is being given to the impact of environmental and human factors and their interactions.

Consequently, risk analysis investigations for the operations of AUVs are growing in significance [13]. AUVs with a propulsion system capable of high-speed movement may lead to additional communication limitations, like the Doppler effect or self-generated noise. For this reason, the communication aptitude of AUVs is also a vital component to consider [15].

The research assesses the efficiency of four steering control approaches PID, FOPID, and neural networks in enhancing the navigation and maneuverability of autonomous undersea vehicles, with a particular focus on the REMUS platform. The structure of the paper is outlined as follows: first, a literature review on AUV control methods, followed by a meticulous explication of the methodology, experimental setup, and outcomes, and ultimately, concluding with a discussion of the implications and future research directions.

## II. System Model and Control Design

This section examines the intricate mechanisms and methodologies utilized in our research to provide a comparative analysis of steering control systems. The principal objective of this study is to scrutinize and contrast three distinct steering control paradigms meticulously: fractional order proportional-integral-derivative (FOPID), proportional-integral-derivative (PID), and neural network (NN) control systems. By comparing these diverse methodologies, we aim to elucidate their subtleties, advantages, and drawbacks within steering control applications.

This study utilized simulation-based methodology to examine the control strategy that we put forward extensively. Using simulation tools, we carefully devised a control approach mirroring real-world implementations. This technique enabled us to investigate various scenarios, systematically manipulate variables, and precisely observe controller response. By utilizing simulation, we obtained valuable insights into three standard control strategies. This has illuminated subtle patterns and disparities that could be very costly to detect through conventional experimentation alone. In our comparative analysis of PID, FOPID, and NN controllers for marine navigation systems, we justify their distinct applications and advantages within the maritime domain. PID controllers have emerged as a dependable choice in marine navigation due to their widespread use and ability to provide precise control [16]–[18]. This is especially obvious in tasks such as regulating the shaft speed of marine electric propulsion systems. Additionally, FOPID controllers, as a more sophisticated modification version of PID, offer improved response dynamics and increased stability, making them promising for improving navigation system performance in varying sea conditions [19]. Furthermore, NN controllers demonstrate adaptability and effectiveness in real-time decision-making processes, finding applications in various maritime scenarios, such as ship berthing, guidance, and heading control systems [20]–[23]. By comparing these three controllers, we aim to provide valuable insights into their strengths and suitability for various aspects of marine craft navigation. Overall, PID, FOPID, and NN controllers are beneficial in marine navigation as they can provide accurate system output control output and have been implemented in various marine navigation problems.

### A. AUV Mathematical Model

Designing the AUV motion model involves analyzing the AUV motion dynamics, which requires a thorough comprehension of the reference axis system. Understanding the reference axis system is a crucial prerequisite for creating the AUV motion model and studying the AUV motion dynamics. The equation of motion is based on six degrees of freedom (DOF) as seen in Figure 1 and Table 1, which is similar to that of a submarine and employs the Earth Fixed Frame (EFF) and Body Fixed Frame (BFF) axes.

The general 6-DOF (Six Degree of Freedom) equations of motion of the AUV consist of the first three equations for translational motion (surge, sway, heave), and the next three equations of motion (roll, pitch, yaw) are for rotational motion [24]–[26], which can be written as (1).

$$\boldsymbol{M}_{RB}\dot{\boldsymbol{v}} + \boldsymbol{C}_{RB}(\boldsymbol{v})\boldsymbol{v} = \boldsymbol{\tau}_{RB} \tag{1}$$

The vectors $\boldsymbol{v} = [v_1 \quad v_2]^T$ comprising of $\boldsymbol{v_1} = [u \quad v \quad w]^T$ and $\boldsymbol{v_2} = [p \quad q \quad r]^T$ denote the linear and angular velocities expressed in BFF. Additionally, $\boldsymbol{\tau} = [\Sigma X \quad \Sigma Y \quad \Sigma Z \quad \Sigma K \quad \Sigma M \quad \Sigma N]^T$ are external moments acting on the AUV. $\boldsymbol{M}_{RB}$ refers to the mass of the AUV's rigid body, which can be expressed as the rigid body mass matrix, as in (2).

$$\boldsymbol{M}_{RB} = \begin{bmatrix} mI_{3\times3} & -mS(\boldsymbol{r_g}) \\ mS(\boldsymbol{r_g}) & I_o \end{bmatrix} \tag{2}$$

Where $I_{3\times3}$ represent $3 \times 3$ identity matrix, $S(\cdot)$ represents a $3 \times 3$ skew-symmetric matrix, as seen in (3). The vector $r_g = [x_g \quad y_g \quad z_g]$ denote the AUV center of gravity.

$$S(\boldsymbol{r_g}) = \begin{bmatrix} 0 & -z_g & y_g \\ z_g & 0 & -x_g \\ -y_g & x_g & 0 \end{bmatrix} \tag{3}$$

$I_o$ is the inertial tensor of the AUV, which is a symmetric and positive definite tensor as in (4).

$$I_o = \begin{bmatrix} I_{xx} & -I_{xy} & -I_{xz} \\ -I_{yx} & I_{yy} & -I_{yz} \\ -I_{zx} & -I_{zy} & I_{zz} \end{bmatrix} \tag{4}$$

The formulation also includes $\boldsymbol{C}_{RB}$ matrix or rigid body Coriolis matrix as in (5).

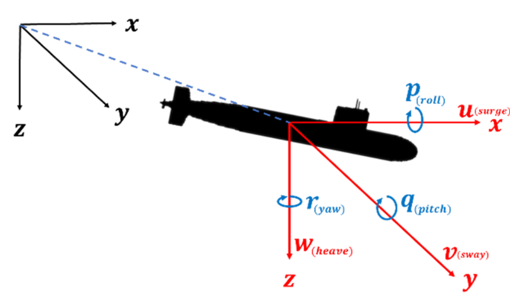


Figure 1. Reference frame of six degrees of freedom of AUV motion (Body fixed frame and earth fixed frame).

TABLE 1
AUV TERMS OF REFERENCE NOTATION

| AUV Motion | Positions/Angle Euler | Linear-Velocities/Angular Velocity | Forces/ Moments |
|---|---|---|---|
| Surge | $x$ | u | $X$ |
| Sway | $y$ | $v$ | $Y$ |
| Heave | $z$ | $w$ | $Z$ |
| Roll | Φ | $p$ | $K$ |
| Pitch | Θ | $q$ | $M$ |
| Yaw | $\psi$ | $r$ | $N$ |

$$\boldsymbol{C}_{RB}(\boldsymbol{v}) = \begin{bmatrix} 0_{3\times3} & -mS(\boldsymbol{v_1}) - mS(\boldsymbol{v_2})S(r_g) \\ -mS(\boldsymbol{v_1}) + mS(\boldsymbol{r_g})S(\boldsymbol{v_2}) & -S(I_o\boldsymbol{v_2}) \end{bmatrix} \quad (5)$$

### B. Steering Model Linearization

When the AUV moves horizontally, changing the rudder deflection causes a yaw moment that alters the heading direction. Steering control depends on three states affecting sway speed($v$), yaw rate ($r$), and yaw angle ($\psi$), with the rudder deflection ($\delta r$) serving as the control input, in the Euler Angle attitude term we can define angular velocity as in (6).

$$\begin{bmatrix} \dot{\phi} \\ \dot{\theta} \\ \dot{\psi} \end{bmatrix} = \begin{bmatrix} 1 & s\phi t\theta & c\phi \\ 0 & c\phi & -s\phi \\ 0 & \frac{s\phi}{c\theta} & \frac{c\phi}{c\theta} \end{bmatrix} \begin{bmatrix} p \\ q \\ r \end{bmatrix} \quad (6)$$

For the purposes of this study, it is assumed that the velocities in the x, y, and z directions ($u$, $w$, p, and $r$) are all equal to zero, as well as the coordinates of the object's center of gravity ($x_g$, $y_g$, and $z_g$). Thus, combining (1), and (6) yields a straightforward matrix equation that represents the simplified linear steering model as in (7).

$$\begin{bmatrix} m - Y_{\dot{v}} & -Y_{\dot{v}} & 0 \\ -N_{\dot{v}} & I_z - N_{\dot{r}} & 0 \\ 0 & 0 & 1 \end{bmatrix} \begin{bmatrix} \dot{v} \\ \dot{r} \\ \dot{\psi} \end{bmatrix} - \begin{bmatrix} m - Y_{\dot{v}} & -Y_{\dot{v}} & 0 \\ -N_{\dot{v}} & I_z - N_{\dot{r}} & 0 \\ 0 & 0 & 1 \end{bmatrix} \begin{bmatrix} \dot{v} \\ \dot{r} \\ \dot{\psi} \end{bmatrix} = \begin{bmatrix} Y_{\delta r} \\ N_{\delta r} \\ 0 \end{bmatrix} [\delta r] \quad (7)$$

The parameter values pertaining to the AUV dynamics are presented in Table 2.

TABLE 2
AUV SPECIFICATION PARAMETERS

| Parameter | Value | Units | Description |
|---|---|---|---|
| $\boldsymbol{I_z}$ | 3.45 | $kg.m^2$ | Momen inertia at CB |
| $\boldsymbol{Y_{\dot{v}}}$ | -35.5 | $kg$ | Added Mass |
| $\boldsymbol{Y_{\dot{r}}}$ | 1.93 | $\frac{kg.m}{rad}$ | Added Mass |
| $\boldsymbol{N_{\dot{v}}}$ | 1.93 | $kg.m$ | Added Mass |
| $\boldsymbol{N_v}$ | -3.18 | $kg$ | Cross-flow Drag |
| $\boldsymbol{N_{\dot{r}}}$ | -4.88 | $\frac{kg.m^2}{rad}$ | Added Mass |
| $\boldsymbol{N_r}$ | -9.40 | $\frac{kg.m^2}{rad^2}$ | Cross-flow Drag |
| $\boldsymbol{N_{\delta_r}}$ | -6.15 | $\frac{kg}{rad}$ | Fin Lift Momen |
| $\boldsymbol{Y_v}$ | -131 | $\frac{kg}{m}$ | Cross-flow Drag |
| $\boldsymbol{Y_r}$ | 0.632 | $\frac{kg.m}{rad^2}$ | Cross-flow Drag |
| $\boldsymbol{Y_{\delta_r}}$ | -3.18 | $\frac{kg}{m.rad}$ | Fin Lift Force |

### C. Fractional Order PID (FOPID)

The combination of controls can address limitations and emphasize the benefits of each component [27]. The standard form of the mathematical model for a PID controller is as (8).

$$u(t) = K_p e(t) + K_i \int_0^t e(t)\, d(t) + K_d \frac{d}{d(t)} e(t) \quad (8)$$

where $u(t)$ represents the output of the PID controller and e(t) denotes the error as in (9). $K_p$, $K_i$, and $K_d$ signify the proportional, integral, and derivative gains for the PID controller. Fractional Order PID (FOPID) is a controller that merges the PID controller with the fractional calculus idea. The FOPID controller mathematical model's general form is presented here [28].

$$u(t) = K_p e(t) + K_i D^{-\lambda} e(t) + K_d D^{\mu} e(t) \quad (9)$$

where $u(t)$ represents the output of the FOPID controller and $e(t)$ denotes the error, where and refer to the order of integral and differential operators, respectively. $K_p$, $K_i$, and $K_d$ correspond to the P= proportional, integral, and derivative gains for the FOPID controller. D is expressed in the fractional differ integral form of Grunwald-Letnikov. From equation (9), five parameters will be tuned separately for the FOPID controller: $K_p$, $K_i$, $K_d$, λ, and μ. The Ziegler-Nichols method can be utilized to determine the values of Kp, Ki, and Kd. The value of λ and μ can be chosen within the range of 0 < λ < 1 and 0 < μ < 1, as noted in reference [28]. It is worth noting that while Mohamed determined the values of λ and μ within the range of 0 < λ < 2 and 0 < μ < 2, as reported in reference [29], another option exists. The λ and μ tuning method developed by Yeroglu and colleagues, as outlined in the reference [30], offers an alternative method to calculate the values of λ and μ.

### D. Neural Network PID

The NN-PID control is a common PID control that employs an artificial neural network to directly adjust the P, I, and D constants. This control utilizes a single neuron structure with three inputs and one output, making it easy to optimize weight adjustments for improved control performance. The block diagram for REMUS AUV's NN-PID control is shown in Figure 2. The inputs for a neuron are $x_1$, $x_2$, and $x_3$ as in (10)-(12), while P, I, and D are weights representing proportional, integral, and derivative constants. The plant control signal's input is $u(t)$. The state converter calculates errors for proportional, integral, and derivative terms using discrete formulas.

$$x_1 = e(t) \quad (10)$$

$$x_2 = e(t) - e(t-1) \quad (11)$$

$$x_3 = e(t) - 2e(t-1) + e(t-2) \quad (12)$$

The control signal is calculated using the following equation: $e(t) = r(t) - ythe\ (t)$ where $e(t)$ is the error at time $k$, $e(t-1)$ is the error at time $(t-1)$, and $e(t-2)$ is the error at time $t-2$. The control signal is calculated by (13).

$$u(t) = u(t-1) + \Big(Pe(t) + I\big(e(t) - e(t-1)\big) + D\big(e(t) - 2e(t-1) + e(t-2)\big)\Big) \quad (13)$$

Using a given learning rate, the backpropagation algorithm optimizes the weights of the neural networks

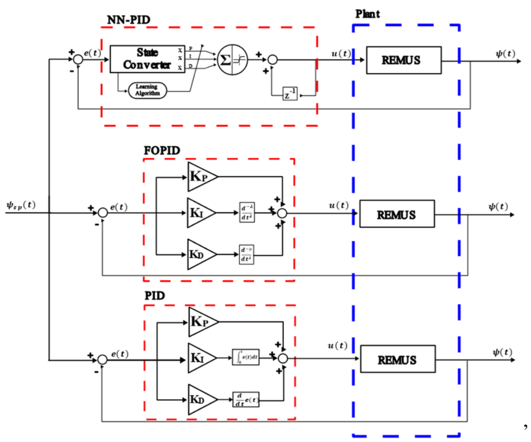


Figure 2. AUV steering control method.

representing P, I, and D. The equation for the input neurons is as (14).

$$Z = \sum_{n=1}^{3} x(t)weight_n(t) = x_1(t)P(t) + x_2(t)I(t) + x_3(t)D(t) \quad (14)$$

Then bipolar sigmoid activation function uses bipolar sigmoid for the output of neuron as in (15).

$$u(t) = \frac{1-e^{-z}}{1+e^{-z}} \quad (15)$$

Backpropagation calculates the error signal ($\delta$) for the neuron input using the chain rule law as in (16).

$$\delta = \left(r(t) - y(t)\right)\left(f'(Z)\right)$$
$$\delta = (r(t) - y(t)(0.5)(1 + u(t))(1 - u(t)) \quad (16)$$

Next, calculate the weight corrections (P, I, D) by inputting α (learning rate) as in (17).

$$\Delta P = \alpha\delta x_1; \Delta I = \alpha\delta x_2; \Delta D = \alpha\delta x_3 \quad (17)$$

And then updating new P, I and D as in (18)-(20).

$$P_{new} = P_{old} + \Delta P \quad (18)$$

$$I_{new} = I_{old} + \Delta I \quad (19)$$

$$D_{new} = D_{old} + \Delta D \quad (20)$$

For the proposed control architecture as in Figure 2. The control architecture implements PID, FOPID, and NN-PID to compare the effectiveness of steering control for a heading problem.

## E. Simulation Setup

The study will utilize rudder deflection input in the time domain. It will comprehensively evaluate and compare the control system parameters response, including Rise Time, Settling Time, Settling Min, Settling Max, Overshoot, Peak, and Peak Time, for each controller response. To thoroughly assess the system performance using various control techniques, this study will employ the heading angle input without modifying the surge, sway, and heave velocities. Three specific scenarios are included in the testing procedure: system response to step inputs, system response to trajectory, and system response to step inputs with disturbances. This methodology allows for a meticulous evaluation, which is crucial for arriving at informed decisions on the most appropriate controller for yaw angle applications about control systems engineering. Additionally, error analysis is conducted for each control strategy utilizing the root mean square error (RMSE) technique to assert with confidence that a model with a lower RMSE indicates better accuracy performance for the controller, enabling users to select the appropriate control strategy.

# III. Result and Discussion

This study evaluated the effectiveness of various steering control methods, including PID, FOPID, and NN-PID, using an extensive analysis that involved measuring rudder deflection input and steady-state error to determine the dynamic behavior of control systems. We determined the dynamic traits of our system by assessing its response in the time domain, paying close attention to response factors such as rise time, overshoot, settling time, and steady-state error, as they are critical in defining the dynamic behavior of control systems.

Three parameters $k_p$, $k_i$, and $k_d$ have been adjusted using the Ziegler-Nichols method for the design of the PID controller. The parameter values for these three parameters are as follows: $k_p = 2.1039$, $k_i = 0.3627$, and $k_d = 1.4506$. For FOPID, the tuning of μ and λ parameters is based on the results obtained in the form of $\lambda = 1.3$ and $\mu = 1.2$, respectively. Regarding NN-PID, the weight values for $k_p$, $k_i$, and $k_d$were initialized randomly. However, these values would be fine-tuned directly to reduce the error rate. The learning rate for this system is set to 0.01.

## A. System Response to Step

During the simulation with a step input, the set point was set to 1 radian. The rise time response outcomes of the PID and FOPID controllers were 0.7136 and 0.4725 seconds, respectively. The settling time results indicated that the PID response was slower than that of the FOPID controller, with each controller taking 4.0698 and 3.2218 seconds, respectively. Meanwhile, the response of the NN-PID controller is slower than that of the two previous controllers, with a rise time of 2.1953 seconds and a settling time of 12.2227 seconds. This delay is attributed to the required learning time for the NN-PID controller. A comprehensive data presentation is available in Table 3.

The graph in Figures 3(a) and 3(b) depicting the controller's response provides a visual representation of

Table 3
Controller Step Response

| Parameters | FOPID | NN-PID | PID |
|---|---|---|---|
| **Rise Time (sec)** | 0.7136 | 2.1953 | 0.4725 |
| **Settling Time (sec)** | 3.2218 | 12.2227 | 4.0698 |
| **Settling Min (rad)** | 0.9099 | 0.8776 | 0.928 |
| **Settling Max (rad)** | 1.046 | 1.0029 | 1.0447 |
| **Overshoot (%)** | 4.4485 | 0.3022 | 4.4658 |
| **Peak (rad)** | 1.046 | 1.0029 | 1.0447 |
| **Peak Time (sec)** | 1.8214 | 4.5502 | 0.9284 |

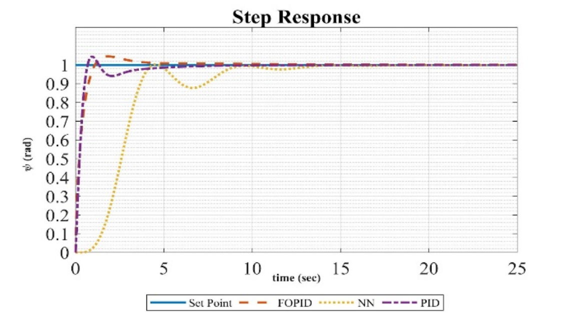


(a)

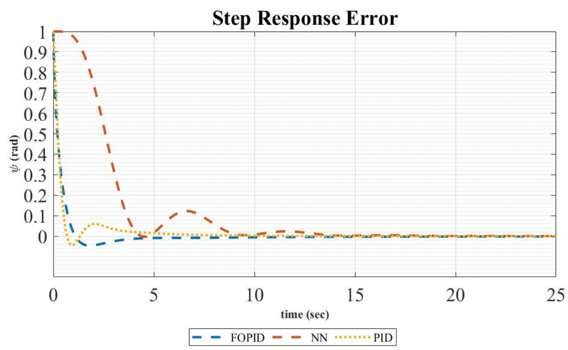


(b)

Figure 3. (a) Step response; (b) Step response RMSE.

the system's behavior. Based on the simulation response of three controllers, NN-PID outperforms PID and FOPID in terms of overshot values. NN-PID only produces an overshot of 0.3022% while PID has a higher percentage of 4.4658% and FOPID has 4.4485%.

## B. System Response to Trajectory

To further evaluate the effectiveness of each control method, trajectory testing was conducted. The reference is initially set to 0 radians for the first 20 seconds, then increases to 0.4 radians from the 20th second to the 45th second. From 45 to 75 seconds, it's reduced to 0.3 radians, and then decreases by 0.2 radians after the 75th second until the end of the simulation. The controller's response is visible in Figures 4(a) and 4(b).

The NN-PID control consistently generates slower responses than the other two, with PID and FOPID showing equal speed. This is due to the NN-PID control requiring a learning process to adjust the weight of the PID constant. This is due to the NN-PID control requiring a learning process to adjust the weight of the PID constant. Regarding overshot, PID and FOPID produce higher values than NN-PID. This is due to the NN-PID control requiring a learning process to adjust the weight of the PID constant. In contrast, NN-PID causes more undershoots than the other two.

## C. System Response with Disturbance

The controller's robustness is tested by introducing disturbances into the system. Initially, the system is given a 1 rad reference, and once reaching a steady state, a 0.1 rad disturbance is added to the output between the 15th and 30th seconds. Figure 5(a) exhibits the control response under disturbance, while Figure 5(b) portrays the reference error. All control methods effectively manage disturbances by returning the response to the reference value. However, NN-PID control operates at a slower pace than other methods discussed previously.

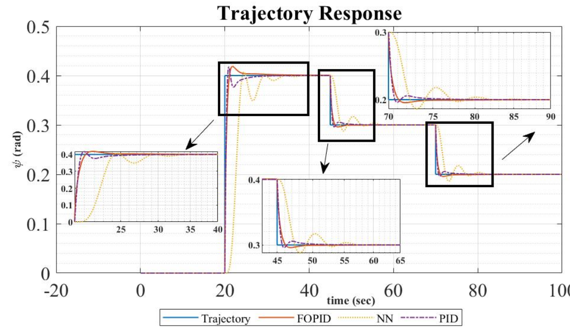


(a)

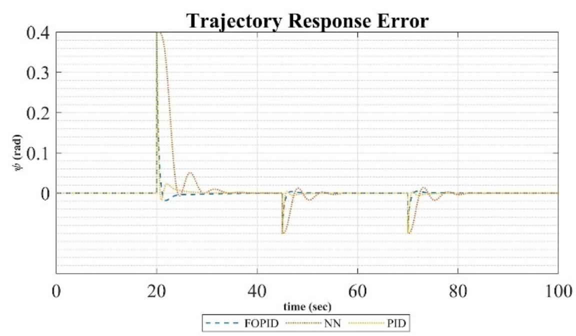


(b)

Figure 4. (a) Trajectory response; (b) Trajectory response RMSE.

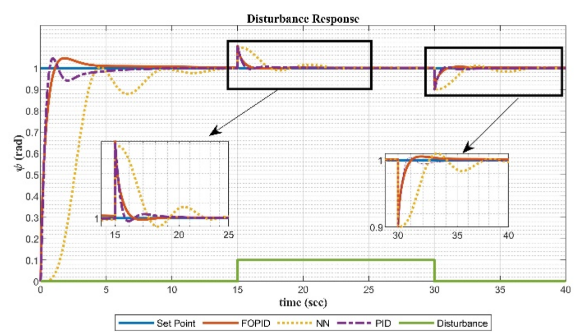


(a)

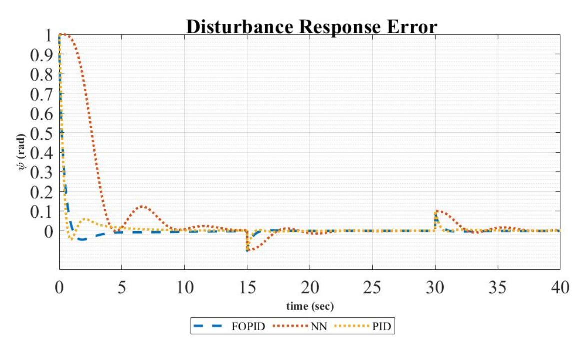


(b)

Figure 5. (a) Response to disturbances; (b) RMSE for response to disturbances.

TABLE 4
ROOT MEAN SQUARE ERROR (RMSE)

| Root Mean Square Error | | | |
|---|---|---|---|
| **Controller** | **Step** | **Trajectory** | **Disturbance** |
| **FOPID** | 0.3211 | 0.7427 | 0.2403 |
| **NN-PID** | 0.5143 | 0.7827 | 0.3842 |
| **PID** | 0.3309 | 0.7440 | 0.2476 |

## IV. ROOT MEAN SQUARE ERROR (RMSE)

Table 4 presents a comparison of errors generated from all testing scenarios. FOPID has an advantage in this regard. The step test and trajectory produce RMSE of 0.3211 and 0.7427, respectively. FOPID robustness to disturbances produces an RMSE of 0.2403. The RMSE produced by PID control is not significantly different from FOPID, with each producing RMSEs of 0.3309, 0.7440, and 0.2476 for the three test scenarios, respectively. Meanwhile, due to the online learning process, the RMSE of NN-PID is consistently higher, with values of 0.5143, 0.7827, and 0.3842 for the step response, trajectory, and testing with disturbances, respectively.

## V. CONCLUSION

PID, FOPID, and NN-PID have been employed as control methods for steering the Remus AUV. Each technique performs well, but FOPID achieves the fastest response time, followed by PID. In contrast, NN-PID results in a slower response time due to its online learning process. Consequently, the error generated by NN-PID is greater than that of PID and FOPID. Nevertheless, NN-PID can reduce overshoots more effectively than the other two methods. In comparison, FOPID improves settling time and produces the smallest error by adding parameters λ and μ, proven to enhance control performance beyond that of PID controllers and NN-PID. Future research will test each control method's robustness, particularly NN-PID with its online learning concept, across varied scenarios.

## DECLARATIONS

### Conflict of Interest

The authors have declared that no competing interests exist.

### CRediT Authorship Contribution

Osen Fili Nami: Conceptualization, Methodology, Software, Writing-Original draft; Afif Widaryanto: Methodology, Simulation, Investigation, Writing-Original draft; Muhammad Putra Rasuanta: Visualization, Writing-Review and Editing; Tinova Pramudyaa: Writing-Review and Editing; Muhammad Yusha Firdaus: Writing-Review and Editing; Peni Laksmita Widati: Writing-Review and Editing; Sakinah Puspa Anggraeni: Writing-Review and Editing; Hanifah Dwiyanti: Writing-Review and Editing Maristya Rahmadiansyah: Supervision, Funding Acquisition; Michael Andreas Purwoadi: Conceptualization, Supervision; Sasono Rahardjo: Conceptualization, Supervision.

### Funding

This publication was funded by the *Rumah Program Sistem Otonom Kendaraan Listrik 2023* with research entitled "Control and Navigation System of Autonomous Underwater Vehicle (AUV) based on Simultaneous Localization and Mapping (SLAM) Equipped with Hybrid Sensor Fusion Method for Underwater Biodiversity Mapping".

### Acknowledgment

The authors gratefully acknowledge the support of the National Research and Innovation Agency (BRIN) of Indonesia, particularly the Research Organization for Electronics and Informatics.

## REFERENCES

[1] B. Jiang, Z. Xu, S. Yang, Y. Chen, and Q. Ren, "Profile autonomous underwater vehicle system for offshore surveys," *Sensors*, vol. 23, no. 7, Apr. 2023, Art. no. 3722, doi: 10.3390/s23073722.

[2] J. González-García, A. Gómez-Espinosa, E. Cuan-Urquizo, L. G. García-Valdovinos, T. Salgado-Jiménez, and J. A. Escobedo Cabello, "Autonomous underwater vehicles: localization, navigation, and communication for collaborative missions," *Appl. Sci.*, vol. 10, no. 4, Feb. 2020, Art. no. 1256, doi: 10.3390/app10041256.

[3] P. G. Fernandes, P. Stevenson, A. S. Brierley, P. G. Fernandes, P. Stevenson, and A. S. Brierley, "Not to be cited without prior reference to the author AUVS as research vessels: the pros and cons."

[4] A. Monterroso Muñoz, M. J. Moron-Fernández, D. Cascado-Caballero, F. Diaz-del-Rio, and P. Real, "Autonomous underwater vehicles: identifying critical issues and future perspectives in image acquisition," *Sensors*, vol. 23, no. 10, May 2023, Art. no. 4986, doi: 10.3390/s23104986.

[5] Z. Milosevic, R. A. Suarez Fernandez, S. Dominguez, and C. Rossi, "Guidance for autonomous underwater vehicles in confined semistructured environments," *Sensors,* vol. 20, no. 24, Dec. 2020, Art. no. 7237, doi: 10.3390/s20247237.

[6] Y. Chen, Y. Bian, Q. Cui, L. Dong, B. Xu, and M. Hu, "LTVMPC for dynamic positioning of an autonomous underwater vehicle," in *Proc. 2021 5th CAA Int. Conf. Vehicular Control and Intelligence,* 2021. doi: 10.1109/CVCI54083.2021.9661196.

[7] J. G. Bellingham, "Platforms: autonomous underwater vehicles," *Encyclopedia of Ocean Sciences*. Academic Press, pp. 473–484, 2009, doi: 10.1016/B978-012374473-9.00730-X.

[8] R. B. Wynn *et al.*, "Autonomous underwater vehicles (AUVs): their past, present and future contributions to the advancement of marine geoscience," *Mar. Geol.*, vol. 352, pp. 451–468, Jun. 2014, doi: 10.1016/j.margeo.2014.03.012.

[9] D. Li and L. Du, "AUV trajectory tracking models and control strategies: a review," *J. Marine Sci. Eng.,* vol. 9, no. 9, Sep. 2021, Art. no. 1020, doi: 10.3390/jmse9091020.

[10] D. Antonov, L. Kolganov, A. Savkin, E. Chekhov, and M. Ryabinkin, "Navigation and motion control systems of the autonomous underwater vehicle," *EUREKA Phys. Eng.,* vol. 2020, no. 4, pp. 38–50, 2020, doi: 10.21303/2461-4262.2020.001361.

[11] S. Mostafa, Y. Z. Elhalwagy, M. A. H. AboZied, and A. M. Kamel, "Control system design for steering and depth subsystems of autonomous underwater vehicle," in *J. Phys. Conf. Ser.*, 2021, vol. 1721, no. 1, Art. no. 012031, doi: 10.1088/1742-6596/1721/1/012031.

[12] T. Xing, X. Wang, K. Ding, K. Ni, and Q. Zhou, "Improved artificial potential field algorithm assisted by multisource data for AUV path planning," *Sensors*, vol. 23, no. 15, 2023, Art. no. 6680, doi: 10.3390/s23156680.

[13] X. Chen, N. Bose, M. Brito, F. Khan, B. Thanyamanta, and T. Zou, "A review of risk analysis research for the operations of autonomous underwater vehicles," *Reliab Eng Syst Saf*, vol. 216, Dec. 2021, Art. no. 108011, doi: 10.1016/j.ress.2021.108011.

[14] L. An, Y. Li, J. Cao, Y. Jiang, J. He, and H. Wu, "Proximate time optimal for the heading control of underactuated autonomous underwater vehicle with input nonlinearities," *Appl. Ocean Res.*, vol. 95, Feb. 2020, Art. no. 102002, doi: 10.1016/j.apor.2019.102002.

[15] Y. Yang, Y. Xiao, and T. Li, "A survey of autonomous underwater vehicle formation: performance, formation control, and communication capability," *IEEE Commun. Surveys Tutorials*,

vol. 23, no. 2, pp. 815–841, 2021. doi: 10.1109/COMST.2021.3059998.

[16] X. Zhang, X. Xu, X. Xu, P. Hou, H. Gao, and F. Ma, "Intelligent adaptive PID control for the shaft speed of a marine electric propulsion system based on the evidential reasoning rule," *Mathematics*, vol. 11, no. 5, Mar. 2023, Art. no. 1145, doi: 10.3390/math11051145.

[17] A. Saxena, J. Kumar, V. Kumar Deolia -, R. Agrawal -, and T. K. Sethuramalingam, "Fuzzy logic controller based ship navigation system," in *J. Phys. Conf. Ser.*, vol. 1850, no. 1, Jan. 2020, Art. no. 012113, doi: 10.1088/1742-6596/1850/1/012113.

[18] T. A. Tran, "Analysis of the PID controller for marine diesel engine speed on simulink environment," in *Proc. 2020 Int. Conf. Electrical Engineering and Control Technol.,* Dec. 2020. doi: 10.1109/CEECT50755.2020.9298679.

[19] A. M. Nassef, M. A. Abdelkareem, H. M. Maghrabie, and A. Baroutaji, "Metaheuristic-based algorithms for optimizing fractional-order controllers—a recent, systematic, and comprehensive review," *Fractal Fract.*, vol. 7, no. 7, Jul. 2023, Art. no. 553, doi: 10.3390/fractalfract7070553.

[20] N. K. Im and V. S. Nguyen, "Artificial neural network controller for automatic ship berthing using head-up coordinate system," *Int. J. Nav. Archit. Ocean Eng.,* vol. 10, no. 3, pp. 235–249, May 2018, doi: 10.1016/j.ijnaoe.2017.08.003.

[21] N. A. J. Witt, R. Sutton, and K. M. Miller, "A track keeping neural network controller for ship guidance," *IFAC Proc.*, vol. 28, no. 2, pp. 385–392, May 1995, doi: 10.1016/S1474-6670(17)51698-5.

[22] T. T. Le, "Ship heading control system using neural network," *J. Marine Sci. Technol.*, vol. 26, pp. 963–972, Sep. 2021, doi: 10.1007/s00773-020-00783-w.

[23] Y. A. Ahmed, M. A. Hannan, and K. H. Siang, "Artificial neural network controller for automatic ship berthing: challenges and opportunities," *Marine Syst. Ocean Technol.*, vol. 15, pp. 217–242, Dec. 2020, doi: 10.1007/s40868-020-00089-x.

[24] M. Renilson, *Submarine Hydrodynamics*. Cham: Springer International Publishing, 2015. doi: 10.1007/978-3-319-16184-6.

[25] T. I. Fossen, "A nonlinear unified state-space model for ship maneuvering and control in a seaway," *Int. J. Bifurc. Chaos*, vol. 15, no. 9, pp. 2717–2746, 2005, doi: 10.1142/S0218127405013691.

[26] C. Yang and B. Eng, "Modular modeling and control for autonomous underwater vehicle (AUV)," M.S. thesis, Nat. Univ. Singapore, 2007. Accessed: Aug. 26, 2024. [Online]. Available: https://core.ac.uk/reader/48625100

[27] K. Ogata, *Modern Control Engineering,* Pearson, 2010.

[28] A. Tepljakov, E. Petlenkov, and J. Belikov, "Fractional-order calculus based identification and control of linear dynamic systems," M.S. thesis, Tallinn Univ. Tech., 2011. Accessed: Aug. 26, 2024. [Online]. Available: https://a-lab.ee/edu/theses/defended/52

[29] M. J. Mohamed and M. A. Khashan, "Comparison between PID and FOPID controllers based on particle swarm optimization," 2014. Accessed: Aug. 26, 2024. [Online]. Available: https://www.researchgate.net/publication/260417316

[30] C. Yeroglu, C. Onat, and N. Tan, "A new tuning method for pi λ d µ controller," in Proc. *2009 Int. Conf. Electrical and Electronics Engineering,* 2009, doi: 10.1109/ELECO.2009.5355344.